Journal of Solid State Chemistry 184 (2011) 877–880

Contents lists available at ScienceDirect

Journal of Solid State Chemistry

journal homepage: www.elsevier.com/locate/jssc

Compositionally controlled metal–insulator transition in $Tl_{2-x}In_xTeO_6$

Theeranun Siritanon, A.W. Sleight, M.A. Subramanian*

Department of Chemistry, Oregon State University, Corvallis, OR 97331-4003, USA

ARTICLE INFO

Article history:
Received 11 December 2010
Received in revised form
3 February 2011
Accepted 11 February 2011
Available online 19 February 2011

Keywords:
Oxides
Solid solution
Electrical properties
Metal–insulator transition
Percolation

ABSTRACT

Tl_2TeO_6 and In_2TeO_6 are both known to crystallize in the Na_2SiF_6-type structure. We find Tl_2TeO_6 is metallic, whereas In_2TeO_6 is an insulator. We have prepared a complete $Tl_{2-x}In_xTeO_6$ series in a search for a compositionally controlled metal–insulator transition that might be expected if a complete solid solution can be obtained. Unit cell edges and volume vary monotonically with no indication of a miscibility gap. The metal–insulator transition occurs at an x value of about 1.4, which can be rationalized on a percolation model. No superconductivity could be detected down to 5 K.

1. Introduction

Superconductivity frequently appears at a metal–insulator boundary as one varies the composition. One of the classical examples is the discovery of superconductivity in $BaBi_{1-x}Pb_xO_3$ perovskites, where the dilution of an s^1 by an s^0 cation disrupts the Bi disproportionation resulting in metallic properties at x value of about 0.25. Superconductivity with a T_c as high as 13 K occurs just on the metallic side of this metal–insulator (MI) boundary [1]. This approach can be used as one of the ways to find new superconductors.

Ternary tellurium oxides with the general formula M_2TeO_6, where M is a trivalent cation reported to adopt to various crystal structures depending on the ionic radius of M. Small M cations, whose radii are in between 0.5 and 0.7 Å (e.g., Cr, Fe, and Rh) tend to form the trirutile structure (space group $P4_2/mnm$) [2]. The Na_2SiF_6 structure (space group $P321$) is formed when radius of M cation is in the range $0.75 < R_M < 0.87$ Å [3]. For larger M cations ($R_M > 0.87$), the orthorhombic La_2TeO_6-type structure (space group $P2_12_12_1$) is formed [4]. Exceptions are Bi_2TeO_6, Tl_2TeO_6, and Yb_2TeO_6. Bi_2TeO_6 forms layer structure due to presence of a stereoactive lone pair of $6s^2$ electrons on Bi^{3+} [5]. The ionic radii of Yb^{3+} (0.868 Å) and Tl^{3+} (0.885 Å) [6] are at the borderline, and it is reported that Yb_2TeO_6 can form both the Na_2SiF_6 [7] and the La_2TeO_6 [8] structures while Tl_2TeO_6 only forms the Na_2SiF_6 structure [9]. Electrical properties of these tellurates are not well studied. Shannon et al. [10] reported that In_2TeO_6 single crystals grown under high pressures (~58 Kbar) exhibit degenerate semiconducting behavior with resistivity on the order of $10^{-2}\ \Omega$ cm, but the preparation at ambient pressure resulted in an insulating compound. It was assumed in their work that the high pressure phase may be oxygen deficient, but no evidence was given [10]. Insulating behavior for polycrystalline In_2TeO_6 has also been reported by Shemirani and Koffyberg [11], who also reported n-type semiconductivity for Sn-doped In_2TeO_6. The crystal structure of the corresponding thallium analog, Tl_2TeO_6, has been investigated [9] but there are no reports on its electrical properties. In this work, we report on the synthesis, characterization and electrical properties of the complete $Tl_{2-x}In_xTeO_6$ solid solution.

2. Experimental

Polycrystalline samples of $Tl_{2-x}In_xTeO_6$ with $x=0$–2 were prepared by solid state reactions. Stoichiometric mixtures of In_2O_3 (Aldrich, 99.99%), Tl_2O_3 (Johnson Matthey, 99.999%), and TeO_2 (Acros organics, 99%) or H_6TeO_6 (Analar, 99.5%) were ground, pressed into pellets and heated at 550–650 °C in covered gold containers for 24 h in air with intermediate grinding. Powder X-ray diffraction data were obtained by a Rigaku MiniFlex II diffractometer using Cu $K\alpha$ radiation and a graphite monochromator. DC electrical resistivities were measured on the pellets by conventional four-probe method in the temperature range 50–300 K using a Quantum Design PPMS (Physical Properties Measurement System). Seebeck coefficients were determined by static method at room temperature. Highly conducting samples were tested for superconductivity down to 5 K.

---

* Corresponding author.
E-mail address: mas.subramanian@oregonstate.edu (M.A. Subramanian).

0022-4596/$ - see front matter © 2011 Elsevier Inc. All rights reserved.
doi:10.1016/j.jssc.2011.02.008

3. Results

To obtain single phase solid solution compositions, thallium-rich samples were heated at a relatively lower temperature (550 °C) to avoid melting and Tl volatilization, whereas indium-rich samples were heated at a higher temperature (650 °C) because a $In_2Te_3O_9$ phase is formed when heating at lower temperatures [12].

Powder X-ray diffraction data showed that the complete solid solution between In_2TeO_6 and Tl_2TeO_6 could be obtained (Fig. 1). All of the powder X-ray diffraction patterns of the $Tl_{2-x}In_xTeO_6$ series could be indexed assuming the Na_2SiF_6 structure (space group: $P321$; hexagonal unit cell in a trigonal space group) where each In/Tl and Te cation is coordinated by six oxygen anions forming a slightly distorted octahedra (Fig. 2). The $(In/Tl)_2O_6$ octahedra share corners with each other, and they share edges with the TeO_6 octahedra. Although the $(In/Tl)_2O_6$ octahedra are connected in three dimensions, there is no direct connectivity between tellurium octahedra as shown in Fig. 2b. Powder X-ray diffraction patterns of intermediate compositions show some peak broadening due to lattice strain caused by the large size difference of the two M cations (Fig. 1). The unit cell parameters were refined by the least squares method using the Unit Cell program [13]. Cell parameters of Tl_2TeO_6 and In_2TeO_6 agree well with the reported values [9,11]. Fig. 3 shows plots of the refined unit cell parameters and cell volumes versus x in $Tl_{2-x}In_xTeO_6$. Cell parameters and cell volumes decreased when In content is increased as the ionic radius of In^{3+} (0.800 Å, 6-fold) is smaller than that of Tl^{3+} (0.885 Å, 6-fold) [6]. Colors of the samples continuously change from dark brown for Tl_2TeO_6 to pale yellow for In_2TeO_6.

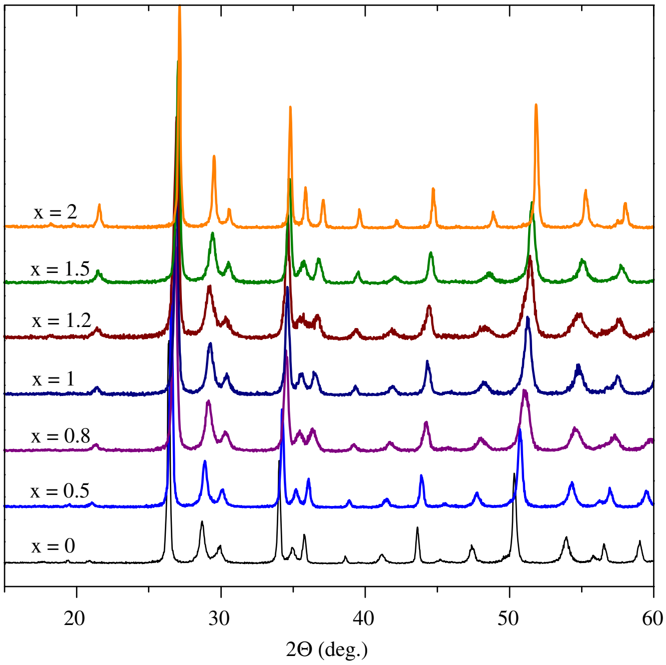

Fig. 1. Powder X-ray data for $Tl_{2-x}In_xTe_2O_6$.

Fig. 4 shows plots of room temperature resistivity and Seebeck coefficients. Samples with $x=1.8$ and 2 were too insulating for a determination of resistivity or the Seebeck coefficient. The general trend is that the resistivity increases with increasing In content and the variation in Seebeck coefficients is consistent with this trend. All measured Seebeck coefficients are negative indicating that the majority of carriers are electrons rather than holes. To exclude the effect of porosity, normalized resistivity $\rho/\rho_{300\ K}$ is plotted versus temperature in Fig. 5. Resistivity and ac magnetic susceptibility measurements of highly conducting compositions ($x<1.5$) show no superconductivity down to 5 K.

4. Discussion

The electronic properties of In_2O_3 are well understood. This oxide is intrinsically an insulator with a direct band gap of 3.75 eV and a smaller indirect gap of 2.6 eV [14,15]. As with CdO, the indirect gap appears to arise from strong mixing between shallow core d states and O 2p states [16,17]. In_2O_3 is easily doped n-type either by oxygen deficiency [14] or by substitution of Sn on In sites [18] to give a highly degenerate transparent conducting oxide. For the simple binary oxides with the cation in the group oxidation state, a very pronounced decrease in band gap occurs on dropping from the In row to the Tl row. In_2O_3 and SnO_2 are transparent insulators, but both Tl_2O_3 and PbO_2 are black and show metallic properties. Single crystals of Tl_2O_3 were reported to have a resistivity of 9×10^{-5} Ω cm at room temperature dropping to 5×10^{-5} Ω cm at 4 K [19]. The magnitude of the resistivity is typical of a metal, but such a weak temperature dependence of resistivity is not expected for a normal metal. It would appear that the band gap in Tl_2O_3 has decreased to zero, that the valence band (O 2p) and conduction band (Tl 6s) have become overlapped, and that Tl_2O_3 is actually a semimetal. Electronic structure calculations and photoemission studies of Tl_2O_3 confirm this description [20]. In the case of Tl_2TeO_6 it appears that the O 2p valence band and the Tl 6s conduction band touch as in the case of Tl_2O_3. The resistivity of Tl_2TeO_6 decreases from 1.88×10^{-3} Ω cm

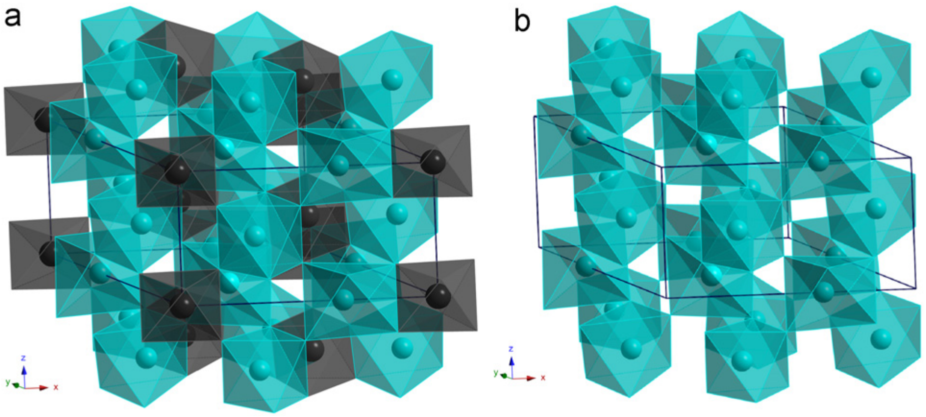

Fig. 2. Structure of In_2TeO_6 and Tl_2TeO_6. Turquoise and black octahedra represent M^{3+} and Te^{6+} octahedral, respectively. Corner shared octahedral network of $M^{3+}O_6$ is shown in (b).

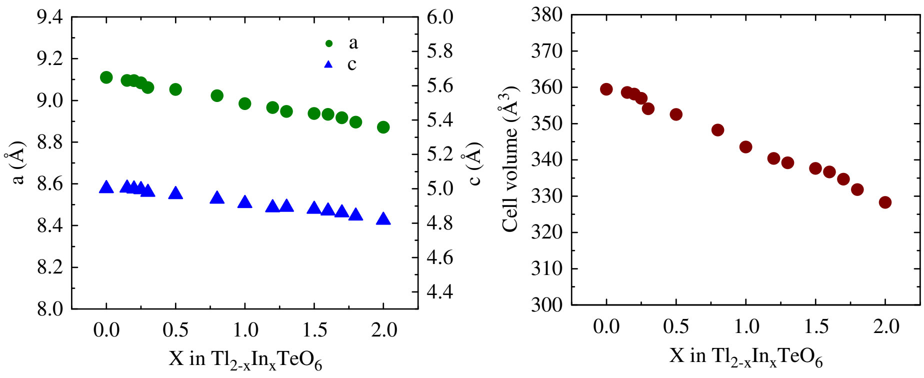

Fig. 3. Lattice parameters (left) and unit cell volumes (right) of $Tl_{2-x}In_xTe_2O_6$ solid solution.

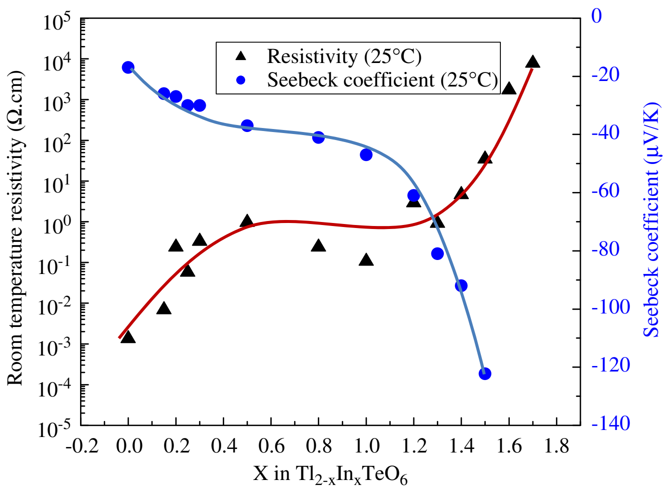

Fig. 4. Room temperature resistivities and Seebeck coefficients of $Tl_{2-x}In_xTe_2O_6$.

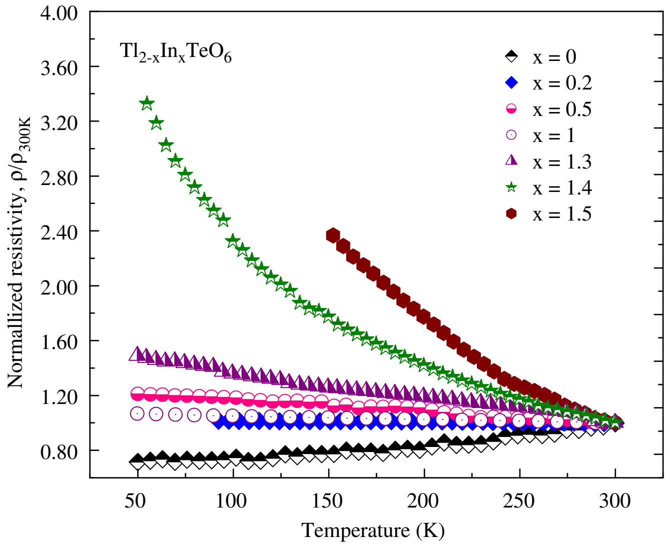

Fig. 5. Normalized resistivities, $\rho/\rho_{300\ K}$ of some representative compositions.

at room temperature to 1.34×10^{-3} Ω cm at 50 K, again a weak temperature dependence indicates a semimetal rather than a normal metal. The situation for oxides of Pb^{4+} is very similar. Both PbO_2 and perovskite $BaPbO_3$ are black and metallic. Band structure calculations indicate that both compounds are semimetals due to an overlap of the O 2*p* valence band and the Pb 6*s* conduction band [21,22]. However in the case of Ba_2PbO_4, the additional Ba has sufficiently stabilized the O 2*p* states such that a small band gap emerges [22]. Stoichiometry may be an issue for PbO_2 and $BaPbO_3$, and it has been very recently suggested that stoichiometric PbO_2 would be a semiconductor with a band gap of 0.7 eV [23]. There apparently is no chemical evidence, such as titration, for such a partial reduction of Pb^{4+}.

A complete solid solution between isostructural oxides is not necessarily expected when one end member is metallic and the other end member is insulating. For example, isostructural metallic RuO_2 and insulating TiO_2 form only a very limited solid solution under equilibrium conditions [24] despite the fact that the radii of Ru^{4+} and Ti^{4+} are nearly the same, 0.62 and 0.605 Å, respectively [6]. However, complete solubility between metallic and insulating compounds is common for ternary oxides. For example, insulating $R_2Ru_2O_7$ compounds (R=rare earth cation) with the pyrochlore structure form complete solid solutions with metallic $A_2Ru_2O_{7-x}$ pyrochlores where A is Pb or Bi [25,26]. Complete solid solutions are also observed between insulating and metallic compounds with the perovskite structure. Examples include $SrTiO_3$–$SrRuO_3$, $ACu_3(Ti_{1-x}Ru_x)_4O_{12}$ (A=Na, Ca, or La), and $R_{1-x}A_xMnO_3$ phases where R is a rare earth cation and A is Ca or Sr [27–29]. One might attempt to rationalize the change from an insulator to a metal as a monotonically decreasing band gap until the gap reaches zero for the metallic state. However, a more realistic model to describe some compositionally controlled MI transitions comes from percolation phenomenon.

A percolation model has been used extensively to describe compositionally controlled MI transitions in composites. Such composites are typically composed of metal particles dispersed in a polymer matrix. When the loading of metallic particles reaches a certain concentration, the bulk properties change from insulating to metallic. The loading necessary for the transition is described by percolation theory [30]. The volume fraction of conducting phase required for high conductivity can be very accurately calculated for ideal systems. For example, assuming the conducting phase to be spheres gives a value of 28.9% as the amount of conducting phase required for complete connectivity and high conductivity [30]. In real systems this critical volume percent can be somewhat higher or lower. The compositionally controlled MI transitions in A_xWO_3 tungsten bronzes can be described using percolation theory. The value of x can be varied over a large range, and it is generally observed that this value must be greater than 0.25 for metallic properties [31]. At lower values of x we can assume that the 5*d* electrons of W produced by the intercalation of the A cations are delocalized over some W atoms, but these electrons remain in the vicinity of the A cations. Thus, the bulk does not exhibit metallic properties. As the concentration of A cations increases, these clusters of delocalized electrons make contact with one another and a change in bulk properties from insulating to metallic occurs. Such a model has been used to explain the compositionally controlled MI transitions in $SrTiO_3$–$SrRuO_3$ and $R_{1-x}A_xMnO_3$ perovskites [27,29].

In the $Tl_{2-x}In_xTeO_6$ solid solution we could assume that metallic conductivity will occur only through Tl–O–Tl linkages. According the percolation theory we can expect continuous Tl–O–Tl linkages will begin to appear at about 30% Tl ($x=1.4$). The exact value depends on assumptions made, such as the nature of likely short range ordering or clustering of In and Tl. In any case, for such a heterogeneous system, an abrupt MI transition is not expected at a precise composition. From a percolation model we expect that resistivity will show a dramatic increase as x increases above about 1.4, and this is observed (Fig. 4). The absolute values of the Seebeck coefficient also show a rapid increase as resistivity increases. Unlike resistivity, the Seebeck coefficient is relatively immune to the impact of grain boundaries. We have a very good fit to a smooth function of the Seebeck coefficient, but there is considerable scatter of the resistivity values. This strongly suggests that grain boundary effects, as well as pellet porosity, have a significant impact on the resisitivity values. This grain boundary contribution is then likely the reason for the very small negative slopes of resisitivity vs. temperature for samples with $x=1.3$ and 1.0 (Fig. 5).

5. Conclusions

A complete series of solid solution between Tl_2TeO_6 and In_2TeO_6 (both crystallizing in the Na_2SiF_6-type structure) has been prepared. Unit cell edges and volume vary monotonically with no indication of a miscibility gap. Tl_2TeO_6 is metallic whereas In_2TeO_6 is an insulator. A compositionally controlled metal–insulator transition occurs at an x value of about 1.4, which could be rationalized on a percolation model. No superconductivity could be detected down to 5 K.

Acknowledgments

The research work done at Oregon State University is supported by a grant from National Science Foundation (DMR-0804167).

References

[1] A.W. Sleight, J.L. Gilson, P.E. Bierstedt., Solid State Commun. 17 (1975) 27.
[2] G. Bayer, Fortschr. Miner. 46 (1969) 41.
[3] J.A. Malone, J.F. Dorrian, O. Muller, R.E. Newnham, J. Am. Ceram. Soc. 52 (1969) 570.
[4] F.W. Hützler, H.-G. Burckhardt, M. Trömel, Z. Kristallogr. 172 (1984) 116.
[5] B. Frit, M. Jaymes, Bull. Soc. Chim. Fr. 1974 (1974) 402.
[6] R.D. Shannon, Acta Crystallogr., Sect. A 32 (1976) 751.
[7] S. Nathanson, J. Inorg. Nucl. Chem 30 (1968) 741.
[8] M. Troemel, F.W. Huetzler, H.G. Burckhardt, C. Platte, E. Muench, Z. Anorg. Allg. Chem. 551 (1987) 95.
[9] F. Bernard, P. Rose, M. Daniele, Mater. Res. Bull. 10 (1975) 1305.
[10] R.D. Shannon, J.L. Gillson, R.J. Bouchard, J. Phys. Chem. Solids. 38 (1977) 877.
[11] B. Shemirani, F.P. Koffyberg, Mater. Res. Bull. 27 (1992) 693.
[12] M.J. Redman, W.P. Binnie, W.J. Mallio, J. Less Common Metals. 23 (1971) 313.
[13] T.J.B. Holland, S.A.T. Redfern, Miner. Mag. 61 (1997) 65.
[14] I. Hamberg, C.G. Granqvist, K.F. Berggren, B.E. Sernelius, L. Engstrom, Phys. Rev. B 30 (1984) 3240.
[15] R.L. Weiher, R.P. Ley, J. Appl. Phys. 37 (1966) 299.
[16] J.E. Jaffe, R. Pandey, A.B. Kunz, Phys. Rev. B 43 (1) (1991) 4030.
[17] Y. Dou, R.G. Egdell, D.S.L. Law, N.M. Harrison, B.G. Searle, J. Phys.: Condens. Matter 10 (1988) 8447.
[18] P.A. Cox, W.R. Flavell, R.G. Egdell, J. Solid State Chem. 68 (1987) 340.
[19] A.W. Sleight, J.L. Gillson, B.L. Chamberland, Mater. Res. Bull. 5 (1970) 807.
[20] P. Glans, T. Learmonth, K.E. Smith, J. Guo, A. Walsh, G.W. Watson, F. Terzi, R.G. Egdell, Phys. Rev. B 71 (2005) 235109.
[21] M. Heinemann, H.J. Terpstram, C. Haas, R.A. deGroot, Phys. Rev. B 52 (1995) 11740.
[22] V.R.R. Medicherla, T. Shripathi, N.P. Lalla, J. Condens. Matter 20 (2008) 035219.
[23] D.J. Payne, R.G. Egdell, D.S.L. Law, P.-A. Glans, T. Learmouth, K.E. Smith, J. Guo, A. Walsh, G.W. Watson, J. Mater. Chem. 17 (2007) 267.
[24] K.T. Jacob, R. Subramanian, J. Phase Equil. Diff. 29 (2008) 136.
[25] Y. Yamamoto, R. Kanno, Y. Takeda, O. Yamamoto, Y. Kawamoto, M. Takano, J. Solid State Chem. 109 (1994) 372.
[26] H. Kobayash, R. Kanno, Y. Kawamoto, T. Kamiyama, R. Izumi, A.W. Sleight, J. Solid State Chem. 114 (1995) 15.
[27] M. Abbate1, J.A. Guevara, S.L. Cuffini, Y.P. Mascarenhas, E. Morikawa, Eur. Phys. J. B 25 (2002) 203.
[28] A.P. Ramirez, G. Lawes, D. Li, M.A. Subramanian, Solid State Commun. 131 (2004) 251.
[29] L. Gor'kov, V. Kresin, J. Super. 13 (2000) 239.
[30] D.R. Baker, G. Paul, S. Sreenivasan, H.E. Stanley, Phys Rev. E66 (2002) 046136.
[31] H.R. Shanks, P.H. Sidles, G.C. Danielson, Adv. Chem. Ser. 39 (1963) 237.